

Dust aerosol radiative effects during a dust event and heatwave in summer 2019 simulated with a regional climate model over Spain

C. Gil-Díaz^(a), M. Sicard^(a,b,c), P. Nabat^(d), M. Mallet^(d), C. Muñoz-Porcar^(a), A. Comerón^(a), A. Rodríguez-Gómez^(a) and D.C.F. Oliveira^(a)

^(a)*CommSensLab, Dept of Signal Theory and Communications, Universitat Politècnica de Catalunya (UPC), Barcelona, 08034, Spain*

^(b)*Ciències i Tecnologies de l'Espai-Centre de Recerca de l'Aeronàutica i de l'Espai/Institut d'Estudis Espacials de Catalunya (CTE-CRAE/IEEC), Universitat Politècnica de Catalunya (UPC), Barcelona, 08034, Spain*

^(c)*Laboratoire de l'Atmosphère et des Cyclones, Université de La Réunion, Saint Denis, 97744, France*

^(d)*Météo-France, CNRM-GAME, Centre national de recherches météorologiques, UMR3589, Toulouse, France*

Lead Author e-mail address: cristina.gil.diaz@upc.edu

Abstract: This study investigates the radiative effects of dust aerosols in the Mediterranean region during a dust event accompanied by a heatwave in summer 2019, using the ALADIN-Climate regional climate model developed at Centre National de Recherches Météorologiques. An evaluation of the simulations performed by ALADIN-Climate is made, showing its ability to reproduce the variability of this dust event. For example, the aerosol optical depth and the shortwave (SW) downward radiative flux at bottom-of-the-atmosphere are compared against observations. Therefore, the dust direct and semi-direct radiative forcings (DRF, SDRF) of dust aerosols provided by ALADIN-Climate model are analyzed at the top-of-the-atmosphere, resulting in a DRF of -0.79 ± 0.76 ($+0.14 \pm 0.07$) W/m^2 and SDRF of $+1.27 \pm 1.34$ ($+0.22 \pm 0.45$) W/m^2 in SW (LW) over Spain. Finally, the changes in the state of the atmosphere associated with the dust aerosols are estimated, showing an increase of atmospheric stability and a possible role of the dust particles as cloud condensation nuclei.

1. Introduction

The Mediterranean region is one of the regions with the highest aerosol load due to air masses carrying many different aerosol types. One of the most common aerosols is mineral dust because of its proximity to the North African deserts [1]. During periods of mineral dust outbreaks, the effect on human health is associated with the biological matter and microorganisms transported by the dust plume that can be harmful to humans [2] and/or with the increase in the particulate matter load at ground level when dust is present [3]. When dust intrusion occurs simultaneously with a heatwave event, its effect on human health gets even worse.

An outstanding event of heatwave coupled with Saharan dust intrusion occurred in June and July 2019. This 14-day event set new high temperature records in several places of Europe, becoming the subject of several studies. In this context, the dust radiative effects and forcings of this dust event during a heatwave are examined with the ALADIN-Climate model during 20th June and 5th July in 2019.

2. ALADIN-Climate model

The present study is carried out with the version 6.4 of the regional climate atmospheric model ALADIN-Climate [4,5], which is used in the CMIP6 and CORDEX exercise. The model lateral boundary conditions are provided by the ERA-INTERIM reanalysis [6]. Two simulations have been carried out using the same initialization of the atmosphere, considering the presence and absence of atmospheric dust particles in the atmosphere (S-DUST/S-NON). The simulations cover the period 20th June to 5th July 2019, during a dust event and heatwave that affected Spain. The domain chosen for this study covers latitudes between 25 and 55° and longitudes between -20 and 20°.

3. Evaluation of ALADIN-Climate simulations

An evaluation of the simulation with dust aerosols during the event is carried out against different available observations. Due to space constraints, only two evaluations will be shown. First, the total AOD measured in different

AERONET stations and with MODIS satellite over Spain is evaluated as shown in Figure 1.

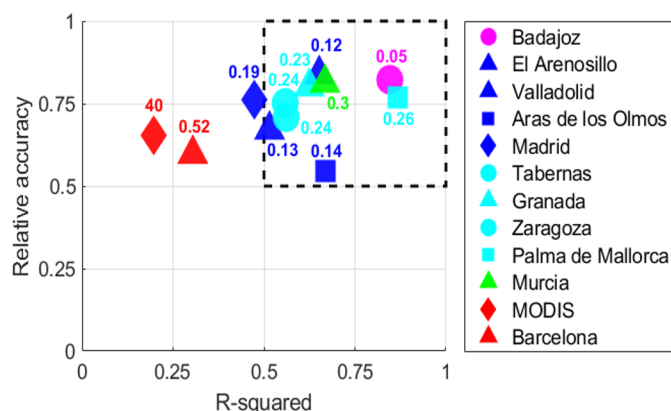


Figure 1. Comparative diagram between the total AOD calculated by the ALADIN-Climate model (S-DUST) and that measured by several AERONET stations and the MODIS satellite over Spain, during the temporal period 23-30th June in 2019. The relative accuracy is 1 - bias, calculated in absolute values. The markers correspond to the different data sets considered. The color of the marker indicates the sum squared error (SSE) interval between simulations and observations, being: magenta 0-0.1; blue 0.1-0.2; cyan 0.2-0.3; green 0.3-0.4; red >0.4. The exact SSE values are written next to each marker. The dashed area marks the region whose relative accuracy and R-squared are higher than 0.5.

In Figure 1 it can be observed that all the points have a relative accuracy value higher than 0.5. On one hand, the Barcelona station is far away from the dashed region, because during the temporal period considered, ALADIN-Climate model overestimates the total AOD measured by the photometer. Therefore, the R^2 is 0.3 and its $SSE=0.52$. On the other hand, MODIS presents a very high value of $SSE=40$ and a low value of $R^2=0.2$, as a consequence of the consideration of the whole Spanish territory. In contrast, the stations where the ALADIN-Climate model best represents the dust event are Badajoz, Palma de Mallorca, Valladolid and Murcia. It is evident that the ALADIN-Climate model best represents the dust event in the east of the Iberian Peninsula, together with the islands of Palma de Mallorca, where the dust load was higher. It also performs well in regions with flat terrain in the center and west peninsular, such as Badajoz.

Afterwards, the downward radiative flux in SW at the Barcelona lidar station is evaluated as shown in Figure 2.

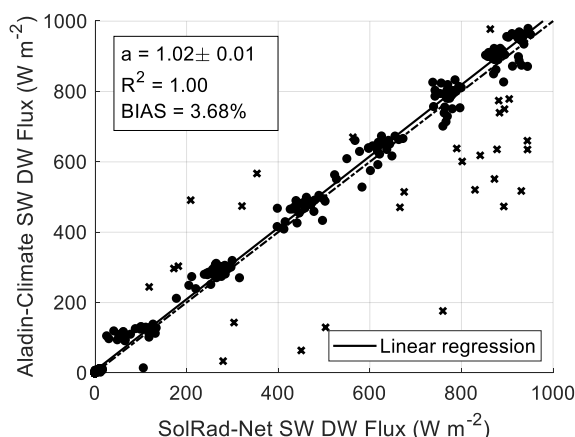


Figure 2. Evaluation of downward radiative fluxes at surface in SW between ALADIN-Climate model (Y-axis) and observations (X-axis), during the period 20th June to 5th July in 2019. The black dashed line is the curve with the slope unity, the black solid line is the linear fitting of the fluxes ($y=ax$, being a the slope and R^2 its determination coefficient). The cross markers indicate when the simulations diverge from the observations in absolute value by more than $100W/m^2$.

Figure 2 shows a good agreement between the simulations performed by ALADIN-Climate model and the observations measured by the pyranometer at surface in Barcelona. The linear regression has a slope $a = 1.02 \pm 0.01$ very close to unity with an $R^2=1$. The averages of the simulations and observations which differ by less than $100 W/m^2$ (point markers) are also relatively similar, being $314W/m^2$ for the simulations and $303 W/m^2$ for the observations. It can also be seen that in 8% of the cases (the cross markers), the ALADIN-Climate model mostly underestimates the downward radiation at the surface. These cases occur mostly in the early hours of the day (6-10hr) during the time period from 20-25th June, revealing the difficulty that the model has in representing the sunrise period during the first days of the dust event.

In this study, additional evaluations of the ALADIN simulations are carried out, such as the evaluation of the daily vertical extinction profiles with the AER product from MPL measurements at the Barcelona lidar station; the evaluation of the dust direct radiative forcings calculated with the GAME model from MPL

and photometer measurements at the Barcelona lidar station (Sicard et al., 2022); the evaluation of surface temperature and pressure in Barcelona with CAMS measurements; the evaluation of vertical profiles of temperature and specific humidity in Barcelona with radiosondes, etc.

4. Direct and Semi-direct radiative forcings

Once the AOD and SW DW fluxes of the ALADIN-Climate model have been evaluated, it is possible to ensure that it represents the dust event fairly accurately and to start analysing the direct and semi-direct forcings at top-of-the-atmosphere produced by the airborne dust particles. The analysis of direct and semi-direct forcing starts at the Barcelona lidar station, where the dust aerosol depth reached values of 0.4 [7], as shown in Figure 3.

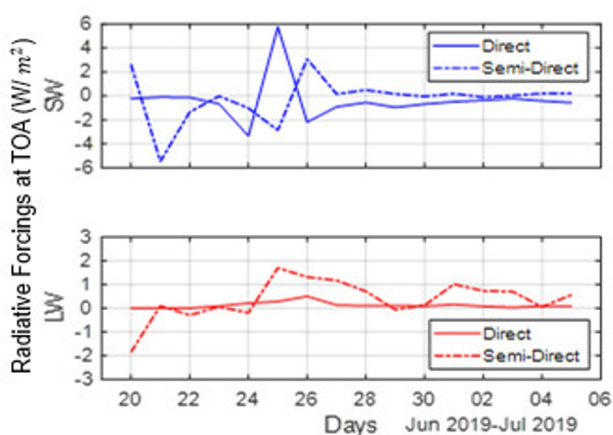


Figure 3. Direct and semi-direct radiative forcing in (top) SW, (bottom) LW at top-of-the-atmosphere, provided by ALADIN-Climate model, in Barcelona during the period 20th June to 5th July in 2019.

Figure 3 shows that the direct radiative forcing is generally negative with a strong positive peak associated with a possible cloud formation. The semi-direct radiative forcing turns from negative to positive after the positive peak of the DRF, resulting in a SW total average of -0.61 ± 2.07 W/m². In LW, the direct forcing is positive and approximately constant, where it reaches its maximum value of $+0.5$ W/m² on 26th June. In contrast, the semi-direct radiative forcing fluctuates between positive and negative values, where its maximum value coincides with the peak of the dust event. This LW effect is also probably related to changes in

cloud cover by dust particles. On average, the LW total radiative forcing is 0.491 ± 0.91 W/m².

Then, the direct and semi-direct radiative forcing at top-of-the-atmosphere over Spain is analyzed, as shown in Figure 4.

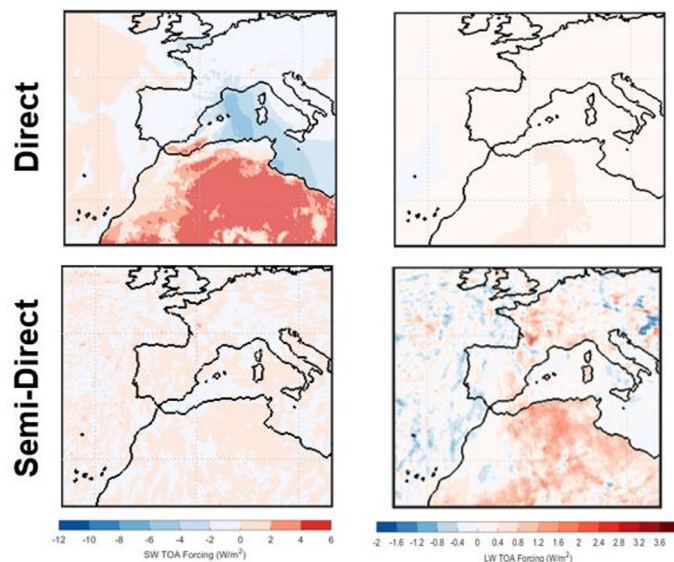


Figure 4. Averages of (top) direct and (bottom) semi-direct radiative forcing in (left) SW, (right) LW at top-of-the-atmosphere, provided by ALADIN-Climate model, during the period 23-30th June in 2019.

Figure 4 shows that, in SW, the direct radiative forcing is generally negative on the European continent and positive on the African continent, due to the large load of Saharan which absorbs the radiation and consequently warms at top-of-the-atmosphere. The semi-direct radiative forcing counteracts the direct radiative forcing with a magnitude even greater than it, as seen in Barcelona. It results in an average of the SW direct radiative forcing of -0.76 ± 0.38 W/m² and semi-direct radiative forcing of $+0.17 \pm 0.32$ W/m² over Spain. In LW, the direct radiative forcing is generally positive in the entire study region and the semi-direct radiative forcing seems correlated to it with negative lows and positive highs and a predominance of positive values in the southeastern part of the region, where the dust load is higher. It results in an average of the LW direct radiative forcing of $+0.14 \pm 0.07$ W/m² and semi-direct radiative forcing of $+0.23 \pm 0.40$ W/m² over Spain.

5. Distinction between dust event and heatwave

Finally, the changes in the state of the atmosphere associated with the Saharan dust

event are analysed, during the time period referred to as "during", from 23th to 30th June in 2019, as shown in Figure 5.

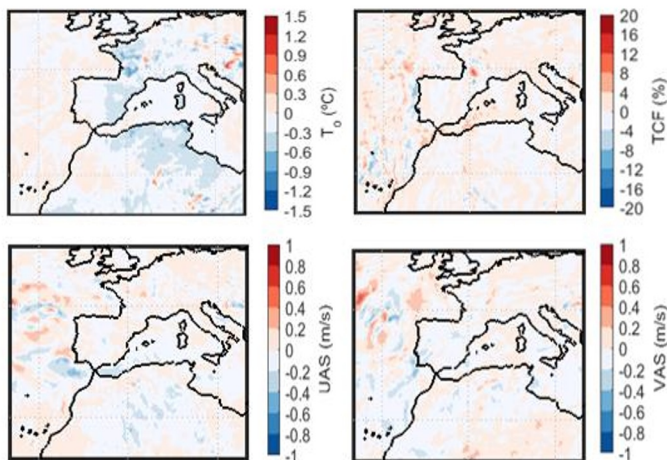


Figure 5. Averages of anomalies of different meteorological variables: surface temperature, total cloud fraction, eastward and northward near-surface wind speed, provided by ALADIN-Climate model, during 23-30th of June in 2019.

Semi-direct forcing is translated into changes in atmosphere state due to the presence of dust aerosols, which absorb or scatter radiation. In Figure 5, it can be observed that the surface temperature has decreased over most of the European and African continent, with minimums in the east, resulting in a surface temperature anomaly averaged over Spain of -0.22°C . This decrease is a consequence of the presence of dust aerosols in the atmosphere that act as a cover, not allowing solar radiation to reach the surface. However, this semi-indirect effect was completely overcome by the heat wave, reaching high temperatures records during this period. On the contrary, the total cloud fraction has been increased in almost all the area considered, resulting in an averaged anomaly of $+0.03\%$ over Spain. This slight increase of cloud growth may be enhanced in some regions by dust particles acting as condensation nuclei [8]. Finally, fluctuations in eastward and northward near-surface wind speed are analyzed. A level decrease in wind speed in both directions appears to dominate over the European and African continents. It results in an average anomaly of -0.04 and -0.02 m/s, respectively. This phenomenon could indicate an increase in atmospheric stability due to dust particles [9], which could lead to a reduction in air quality.

6. References

- [1] Prospero, J.M., Ginoux, P., Torres, O., Nicholson, S.E., and Grill, T.E., "Environmental characterization of global sources of atmospheric soil dust identified with the Nimbus 7 Total Ozone Mapping Spectrometer (TOMS) absorbing aerosol product", *Rev. Geophys.*, 40, 1002, (2002).
- [2] Griffin, D.W.: "Atmospheric movement of microorganisms in clouds of desert dust and implications for human health", *Clin. Microbiol. Rev.*, 20, 459–477, (2007).
- [3] Tobías, A., Pérez, L., Díaz, J., Linares, C., Pey, J., Alastruey, A., Querol, X., "Short-term effects of particulate matter on total mortality during Saharan dust outbreaks: a case-crossover analysis in Madrid (Spain)", *Sci. Total Environ.*, 412-413:386-9, (2011).
- [4] Radu, R., Déqué, M., and Somot, S., "Spectral nudging in a spectral regional climate model", *Tellus*, 60A, 898–910, (2008).
- [5] Farda, A., Déqué, M., Somot, S., Horanyi, A., Spiridonov, V., and Toth, H.: "Model ALADIN as regional climate model for central and eastern Europe", *Stud. Geophys. Geod.*, 54:313–332, (2010).
- [6] Dee, D.P., Uppala, S.M., Simmons, A.J., Berrisford, P., Poli, P., Kobayashi, S., Andrae, U., Balsameda, M.A., Balsamo, G., Bauer, P., Bechtold, P., Beljaars, A.C.M., Van de Berg, L., Bidlot, J., Bormann, N., Delsol, C., Dragani, R., Fuentes, M., Geer, A.J., Haimbergere, L., Healy, S.B., Hersbach, H., Hólm, E.V., Isaksen, L., Kallberg, P., Köhler, M., Matricardi, M., McNally, A.P., Monge-Sanzf, B.M., Morcrette, J.J., Park, B.K., Peubey, C., de Rosnaya, P., Tavolato, C., Thépaut, J.N., Vitart, F., "The ERA-INTERIM reanalysis: configuration and performance of the data assimilation system", *Q. J. R. Meteorol. Soc.*, 137:553–597, (2011).
- [7] Sicard, M., Córdoba-Jabonero, C., López-Cayuela, M.Á., Ansmann, A., Comerón, A., Zorzano, M.P., Rodríguez-Gómez, A., and Muñoz-Porcar, C., "Aerosol radiative impact during the summer 2019 heatwave produced partly by an intercontinental Saharan dust outbreak - Part 2: Long-wave and net dust direct radiative effect", *Atmos. Chem. and Phys.*, 22(3), 1921–1937, (2022).
- [8] Koehler, K.A., Kreidenweis, S.M., DeMott, P.J., Petters, M-D., Prenni, A.J., and Carrico, C.M., "Hygroscopicity and cloud droplet activation of mineral dust aerosol", *Geophys. Res. Lett.*, 36, L08805, (2009).
- [9] Nabat, P., Somot, S., Mallet, M., Sevault, F., Chiacchio, M., and Wild, M. "Direct and semi-direct aerosol radiative effect on the Mediterranean climate variability using a coupled regional climate system model", *Clim. Dyn.*, 44(3–4), 1127–1155.